URSI AP-RASC 2019, New Delhi, India; 09 - 15 March 2019

Computation of Slope Diffraction by Modified Edge Representation (MER) Equivalent Edge Currents (EECs) Line Integration

Maifuz Ali[(1)], Makoto Ando[(2)]
(1) Electronics and Communication Enggineering, IIIT Naya Raipur, India, E-mail: maifuzali@hotmail.com
(2) National Institute of Technology, Higashi Asakawa, Hachioji, Tokyo, Japan, E-mail: ando@kosen-k.go.jp

Abstract

Equivalent edge currents (EECs) line integration to compute the diffracted field has the advantage of less requirement of computation time and resources. The methods of EECs present some ambiguity in the definition of currents at general edge points which do not satisfy the diffraction law. Modified edge representation (MER) is an unique concept for a complete definition of EEC. The line integration of MER EEC results uniform and accurate fields everywhere including geometrical boundaries. Here, MER EECs has been used to compute the diffracted field from the slope of the incident field. The dipole wave scattering from flat circular disk is considered as the numerical examples.

1 Introduction

Physical Optics (PO) is an asymptotic high frequency numerical method based on surface currents. In PO, the scattering fields are obtained by surface integration of surface electric current density, which are performed numerically in general. Since the reduction of the surface integral to line one provides the great saving of the numerical computation time, it has been investigated for long time by many workers in both exact [1–4] and asymptotic manners [5,6].

PO surface integration is reduced to PO MER equivalent edge currents (EECs) line integration in [7] where EECs for physical optics (PO) components at general points are obtained by utilizing the fictitious edges and PO diffraction coefficient. In PO, fringe wave is neglected, If the fringe wave diffraction coefficients added with the PO diffraction coefficients, the diffraction coefficient takes the form of GTD diffraction coefficient given by Keller in [8, eq. (2)] and this MER EECs technique with GTD diffraction coefficient is known as GTD MER. As PO MER is derived directly from PO surface integration, PO MER and hence GTD MER gives the slope effects of the incident field without any extra computation unlike UTD [9, eq. (13-110)]. The slope wave diffraction is a higher order diffraction and it becomes more significant when the incident field at the point of diffraction vanishes. In this paper GTD MER is used to compute the slope wave diffraction and computation of diffracted field of dipole wave from circular disk is considered as the numerical example. Method of moments based numerical electromagnetic code Wipl-D (Wipl-D [10]) is considered as the reference.

2 MODIFIED EDGE REPRESENTATION (MER) FOR THE DEFINITION OF EEC

The method enabling the surface to line integral reduction is the key element in deriving the equivalent edge currents (EECs). A concept of modified edge representation(MER), which extends the definition of EEC for diffraction points to those for general edge points was introduced in [11–13]. Classical Keller's diffraction coefficients were adopted for the computations of the diffracted field as follows.

2.1 Modified Edge Representation $(\widehat{\tau})$

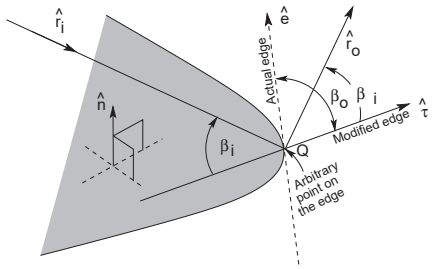

Figure 1. Defination of the modified edge

A fictitious edge $\widehat{\tau}$ is defined to satisfy the diffraction law for the given directions of incidence and observation shown in Fig. 1 and it is simply expressed as:

$$(\widehat{r_o}-\widehat{r_i})\cdot\widehat{\tau}=0 \;\; (\beta_o=\beta_i),\;\; \widehat{n}\cdot\widehat{\tau}=0 \tag{1a}$$

For the observer on ISB/RSB,

$$\widehat{\tau}=\widehat{e} \tag{1b}$$

since the vector $\widehat{\tau}$ in equation (1a) is indefinite on the following geometrical boundaries

$$\widehat{r_o}=\widehat{r_i} \;\; \text{for ISB} \tag{2a}$$
$$\widehat{r_o}=\widehat{r_i}-2\widehat{n}(\widehat{n}\cdot\widehat{r_i}) \;\; \text{for RSB} \tag{2b}$$

Equations (1a) and (1b) determine a unique vector $\widehat{\tau}$ for a given combination of $\widehat{r_i}$ and $\widehat{r_0}$.

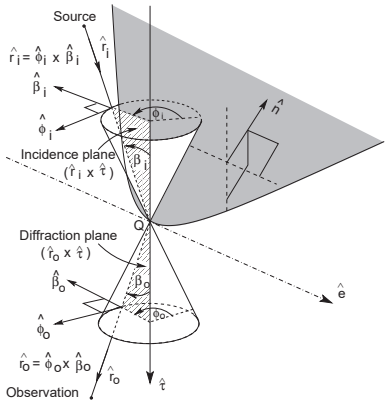

Figure 2. Oblique incidence half-plane diffraction and its top view.

Considering an edge-fixed coordinate system (see Fig. 2), the position of the source and the observer are defined by (r_i, β_i, ϕ_i) and (r_o, β_o, ϕ_o) respectively. The unit vectors $\hat{r_i}$ and $\hat{r_o}$ are in the direction of incidence and diffraction respectively. The unit vector $\hat{e}$ is along the edge and considered according to the counter clockwise direction. The unit vectors $\hat{\beta_i}$ and $\hat{\phi_i}$ are parallel and perpendicular to the edge-fixed plane of incidence respectively. The incident field from the dipole E^i on the point (Q) is decomposed into components parallel to $\hat{\beta_i}$ and $\hat{\phi_i}$ as

$$E^i_{\beta_i}(Q) = \hat{\beta_0'} \cdot \overrightarrow{E}^i(Q) \tag{3a}$$

$$E^i_{\phi_i}(Q) = \hat{\phi_o}' \cdot \overrightarrow{E}^i(Q) \tag{3b}$$

The sign of the modified edge $\hat{\tau}$ defined in (1) is separately determined by that of the following values empirically given in [12]

$$\cos\frac{\phi_o+\phi_i}{2}\cos\frac{\phi_o'+\phi_i'}{2} \quad for\ \phi_o > \pi \tag{4a}$$

$$\cos\frac{\phi_o-\phi_i}{2}\cos\frac{\phi_o'-\phi_i'}{2} \quad for\ \phi_o < \pi \tag{4b}$$

where, ϕ_i, ϕ_i' are the angles of incidence and ϕ_o, ϕ_o' are the angles of diffraction with respect to the modified edge $\hat{\tau}$ and actual edge $\hat{e}$, respectively.

2.2 Equivalent Edge Current and the Diffracted Field

For two polarization in (3a) and (3b), soft and hard boundary conditions are applied and the equivalent edge currents (EECs) along the edge of the scatterer $\hat{e}$ are given by [9, eq. (13-103)],

$$\overrightarrow{I_s} = -\frac{\sqrt{8\pi k}}{\eta k} e^{-j\pi/4} E^i_{\beta_i}(Q) D_s \hat{e} \tag{5a}$$

$$\overrightarrow{I_h} = -\frac{\sqrt{8\pi k}}{\eta k} e^{-j\pi/4} E^i_{\phi_i}(Q) D_h \hat{e} \tag{5b}$$

where D_s & D_h are the diffraction coefficients at the point Q for soft and hard boundary conditions respectively and the Keller's diffraction coefficient of [8, eq. (2)] is

$$D^{GTD}_{s,h} = \frac{-e^{j\pi/4}}{2\sqrt{2\pi k}\sin\beta_i}\left[\sec\left(\frac{\phi_o-\phi_i}{2}\right) \mp \sec\left(\frac{\phi_o+\phi_i}{2}\right)\right] \tag{6}$$

The diffraction fields are expressed as the line radiation integrals of the equivalent edge currents along the peripheries of the scatterers, as follows.

$$\overrightarrow{E^d_s} = \frac{j\eta k}{4\pi}\oint \hat{r_o} \times \left[\hat{r_o} \times \overrightarrow{I_s}\right] \frac{e^{-jk|r_o|}}{|r_o|} dl \tag{7a}$$

$$\overrightarrow{E^d_h} = \frac{j\eta k}{4\pi}\oint \left[\hat{r_o} \times \overrightarrow{I_h}\right] \frac{e^{-jk|r_o|}}{|r_o|} dl \tag{7b}$$

3 Numerical Verification of MER

Numerical verification and validation of GTD MER were detailed in [13]. The diffraction of an infinitesimal dipole wave by rectangular and triangular plates were considered as the numerical examples where edge diffractions and corner diffractions are accounted. The advantages of GTD MER over UTD in terms of corner diffraction were also discussed. As there is no corner in circular disk, diffraction mechanism is comparatively simpler than the rectangular and triangular plates and edge diffraction is the only source of the diffraction. The diffraction of an infinitesimal dipole wave by circular disk as shown in Fig. 3 is considerer to discuss the advantages of MER over UTD in terms of slope wave diffraction.

3.1 Diffraction from a Circular Disk

A dipole along the x-axis is considered at $(0,\ 0,\ 2.5\lambda)$ on a circular disk plate of radius $r_a = 2.5\lambda$ as shown in Fig. 3 and the field patterns at the plane $\phi = 0^\circ$ and $\phi = 90^\circ$ are shown in Fig. 4(a) and Fig. 4(b) respectively. GTD MER computed resulted is compared with the UTD and results using numerical electromagnetic code based on the MoM (Wipl-D [10]). Though there are poles in GTD diffraction coefficient (6) at the reflection shadow boundarie (RSB) and incidence shadow boundarie (ISB), but predicted fields by GTD MER at the shadow boundaries (SBs) are uniform and finite. Also, the fields at and near the geometric acoustics ($\theta = 0^\circ/360^\circ$and 180°) are predicted perfectly.

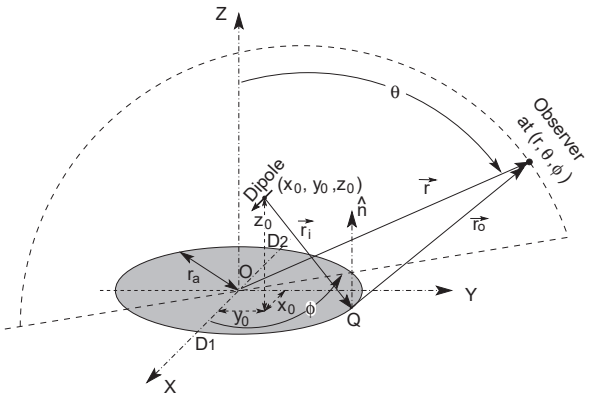

Figure 3. A circular disk illuminated by a dipole.

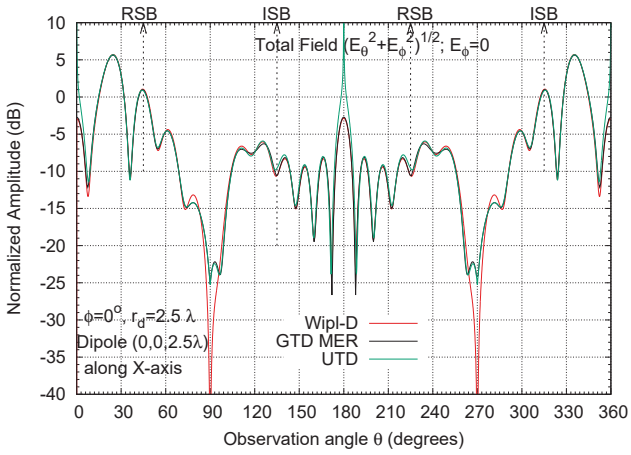

(a)

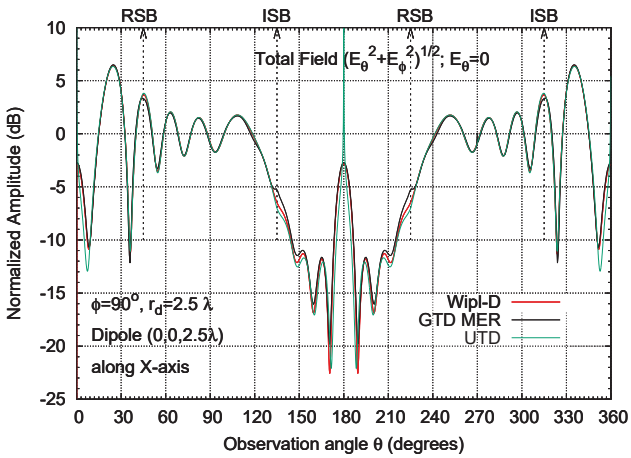

(b)

Figure 4. Total field patterns for a circular disk of $r_a = 2.5\lambda$, dipole at $(0,\ 0,\ 2.5\lambda)$ and the observation at (a) $\phi = 0^\circ$ (b) $\phi = 90^\circ$

4 Slope Diffraction

Next the dipole is turned 45° with x-axis and 135° with z-axis and total field pattern is shown in Fig. 5. The

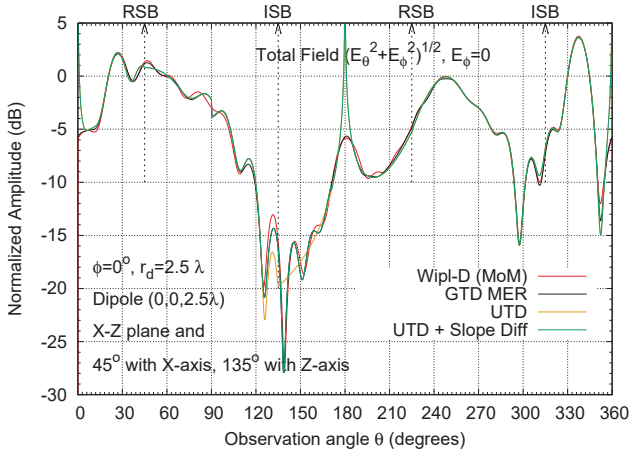

Figure 5. Total field (E_θ) patterns for a circular disk of radius $r_a = 2.5\lambda$, dipole at $(0,\ 0,\ 2.5\lambda)$ in x-z plane making 45° with x-axis and 135° with z-axis and observation at $\phi = 0^\circ$ plane.

GTD MER computed field matches well with Wipl-D results in all angle of observations. The field computed by UTD of [14] shown in the Fig. 5 has disagreement with Wipl-D and GTD MER. The incident field at the diffraction point D_1 $(r_a,\ 0,\ 0)$ is zero but the slope of the incident field is non zero $\left(\frac{\partial E^i_\phi}{\partial n} \neq 0\right)$. Adding slope diffracted field [15] with UTD, results is shown as 'UTD + Slope Diff'. Now the results by UTD with slope diffraction shows very good agreement with Wipl-D. The difference between 'UTD 'and' UTD + Slope Diff' in Fig. 5 shows the slope wave effects. But 'UTD + Slope Diff' yet has disadvantage at geometrical acoustics.

As in planer case, PO MER is the line integration reduction of PO surface integration [11], PO MER includes the effects of the slope of incident field. PO diffraction coefficients added with fringe wave diffraction coefficients give GTD diffraction coefficients [8, eq. (2)]. Hence the technique MER EECs line integrations with GTD diffraction coefficients takes the account of the slope of the incident field at the point of diffraction which is verified through the results in Fig. 5.

5 Conclusion

If incident field at the point of diffraction is zero but slope of this incident field is non zero, slope diffraction gives very important contribution in the field pattern. It is demonstrated by comparing with MoM-based simulator that MER EECs line integration computes efficiently the effect caused by the slope of incident field and no extra computation is needed, like UTD.

Acknowledgment

This work was conducted in part as “the Research and Development for Expansion of Radio Wave Resources ” under the contract of the Ministry of Internal Affairs and Communications, Japan.

References

[1] J. S. Asvestas, “The physical optics fields of an aperture on a perfectly conducting screen in terms of line integrals,” *IEEE Trans. Antennas Propag.*, vol. 34, no. 9, pp. 1155–1159, Sep. 1986.

[2] ——, “Line integrals and physical optics. Part I. The conversion of the Kirchhoff surface integral to a line integral,” *Journal of the Optical Society of America A*, vol. 2, no. 6, pp. 891–895, Jun. 1985.

[3] ——, “Line integrals and physical optics. Part II. The conversion of the Kirchhoff surface integral to a line integral,” *Journal of the Optical Society of America A*, vol. 2, no. 6, pp. 896–902, Jun. 1985.

[4] P. M. Johansen and O. Breinbjerg, “An exact line integral representation of the physical optics scattered field: the case of a perfectly conducting polyhedral structure illuminated by electric hertzian dipoles,” *IEEE Trans. Antennas Propag.*, vol. 43, no. 7, pp. 689 – 696, Jul. 1995.

[5] C. H. Knopp, “An extension of ruschâĂŹs asymptotic physical optics diffraction theory of a paraboloid antenna,” *IEEE Trans. Antennas Propag.*, vol. 23, no. 5, pp. 741–743, Sep. 1975.

[6] A. Michaeli, “Elimination of infinities in equivalent edge currents, Pt.2: Physical optics components,” *IEEE Trans. Antennas Propag.*, vol. 34, no. 8, pp. 1034–1037, Aug. 1986.

[7] K. Sakina and M. Ando, “Mathematical derivation of modified edge representation for reduction of surface radiation integral,” *IEICE Trans. Electronics*, vol. E84-c, no. 1, pp. 74–83, Jan. 2001.

[8] J. B. Keller, “Geometrical Theory of diffraction,” *J.Opt. Soc. Amer.*, vol. 52, pp. 116–130, Feb. 1962.

[9] Constantine A. Balanis, *Advanced Engineering Electromagnetics*. New York: John Wiley & Sons Inc., 1989.

[10] B. M. Kolundzija, J. S. Ognjanovic, and T. K. Sarkar, *WIPL-D: Electromagnetic Modeling of Composite Metallic and Dielectric Structures - Software and User’s Manual*. Boston, London: Artech House, 2000.

[11] T. Murasaki and M. Ando, “Equivalent edge currents by the modified edge representation: Physical optics components,” *Electronics, IEICE Transactions on*, vol. E75-c, no. 5, pp. 617–624, May 1992.

[12] T. Murasaki, M. Sato, Y. Inasawa, and M. Ando, “Equivalent edge currents for modified edge representation of flat plates: Fringe wave components,” *Electronics, IEICE Transactions on*, vol. E76-c, no. 9, pp. 1412–1419, Sep. 1993.

[13] M. Ali, T. Kohama, and M. Ando, “Modified edge representation (MER) consisting of keller’s diffraction coefficients with weighted fringe waves and its localization for evaluation of corner diffraction,” *IEEE Trans. Antennas Propag.*, vol. 63, no. 7, pp. 3158–3167, Jul. 2015.

[14] R. G. Kouyoumjian and P. H. Pathak, “A uniform geometrical theory of diffraction for an edge in a perfectly conducting surface,” *Proc. IEEE*, vol. 62, no. 11, pp. 1448 – 1461, Nov. 1974.

[15] P. H. Pathak, “Techniques for high-frequency problem,” in *Antenna Handbook-Theory, Application and Design*, Y. T. Lo and S. H. Lee, Eds. New York: Van Nostrand Reinhold, 1988, ch. 4, pp. 4–0–4–117.